Journal of Applied Fluid Mechanics, Vol. 17, No. 2, pp. 487-496, 2024.
Available online at www.jafmonline.net, ISSN 1735-3572, EISSN 1735-3645.
https://doi.org/10.47176/jafm.17.02.2071

Vibrational Analysis and Optimization of a Water Injection Pipeline in a High-pressure Plunger Pump

D. Yan[1], C. Zhang[2†], C. Wang[1], T. Zhang[1], C. Wang[1], and F. Sun[1]

[1] *Tarim Oilfield Branch of China National Petroleum Corporation, Xinjiang, 841000, China*
[2] *PetroChina (Xinjiang) Petroleum Engineering Company, Xinjiang, 841000, China*

[†]*Corresponding Author Email: cxling612@126.com*

ABSTRACT

The vibration of water injection pipeline systems in oilfields creates challenges in terms of safe long-term operation. To fully understand the vibration mechanism of plunger-powered high-pressure water injection pipelines, we conducted fluid pressure pulsation calculations and fluid structure coupling modal evaluations using finite element analysis software to study the effects of pressure, pipe length, and pipe clamp on the vibrations. The results indicate that the total displacement increases with increasing pressure, although the magnitude of the increment gradually decreases. The pipe length has a significant impact on the natural frequency. Based on the findings of the present study, we proposed that pipe clamps could be introduced to reduce the vibrations in an existing high-pressure plunger pump water injection pipeline, and the overall design was optimized. Comparative modal analysis revealed the most practical number and position of the pipe clamps to be suitable for a pressure range of 42–70 MPa.

Article History

Received June 5, 2023
Revised September 3, 2023
Accepted September 28, 2023
Available online December 4, 2023

Keywords:

High-pressure water injection pipeline
Pipeline vibration
Modal analysis
Pipe clamp
Vibration reduction optimization

1. INTRODUCTION

High-pressure plunger pump injection has been widely used in gas and oil recovery as an effective, sustainable, and energy-saving extraction technique. However, pipeline system vibration is a common problem affecting high-pressure plunger pump pipes. Pipeline vibration can cause various issues for the pipeline system (e.g., noise, fatigue, leakage, local component loosening, and instrumentation failure), which can impact the pipeline system's long-term operation and safety. Therefore, it is crucial for engineers to understand and solve pipeline vibration issues.

As connected systems, fluid pipelines comprise complicated vibration-triggering elements, which makes it difficult to use a single theorem to handle different pipeline constitution systems. As a result, academics have carried out a significant amount of theoretical and experimental research. The pipeline vibration issue was initially studied by Ashley and Haviland (1950) using a beam model. The dynamic characteristics of cantilever-linked pipes were subsequently explored, and the related Lagrangian and Hamilton equation formulations were established by Housner (1952) and Benjamin (1961), respectively. The Timoshenko beam was employed by Paidoussis & Laithier (1976) to examine the stability of short pipelines. Later, the basic frequency characteristics of pipes with solid supports at both ends, and pipes with concentrated masses were examined by Gregory and Paidoussis (1996) and Long (1955), respectively. Researchers have recently begun to focus on the relationship between fluid-solid interactions and pipe vibrations. Paidoussis (2008) examined the effects of gravity, material damping, and viscous damping on the nonlinear response of pipe systems and developed a dynamic equation for solving this nonlinear response. A numerical model of the nonlinear dynamics of the mutual coupling between the fluids was introduced by Lee et al. (1995), along with the nonlinear response of a pipe. However, this model was limited because the equation must consider numerous factors, such as Poisson's coupling, the fluid's centrifugal force, and the fluid's Gauche force, among others. However, the nonlinear response of the pipeline system is significantly impacted by these elements. The dynamics of a fluid conveyed by a pipeline, as well as the continuous and beam modes of a fluid carried by a cantilever, were explored by Sarkar and Paidoussis (2004). Using the embedded boundary technique and treating the fluid and the structure as a single dynamical system, Yang et al. (2008) investigated the fluid-structure coupling of a rigid structure placed on an elastic base. Tijsseling (2007) created a mathematical model to characterize the features of water-injection pipes while accounting for the coupling between the fluid inside the pipe and the pipe wall; however, the model is only appropriate for thick-walled pipelines. Computations involving a liquid-filled straight pipe with a flange were performed by Finnveden (1997) using a finite element method. They examined the impact of flanges on the

modal frequencies of the pipe system at low frequencies. Long-term excessive vibration of pipeline systems was shown to cause fatigue and micro-motion wear (Azizian & Torrado, 2016) based on case studies of various vibration sources. According to Zhi et al. (2016), the vibration caused by low-frequency and high-amplitude flow results in high cyclic stress and high cyclic fatigue failure because the flow in a pipe produces non-periodic random excitation, which means resonance does not become a critical factor for pipeline failure. in 2014, Sunil and Raghunandana investigated how mechanical resonance affected excessive pipeline vibration. This topic was also explored in terms of fluid-solid coupling, tubing, and two-phase flow by Miwa et al. (2015). According to Li et al. (2012), the fluid-solid coupling effect improves the flow transport pipeline system's natural frequency. Using ANSYS software and a fluid-solid coupling approach, Xie et al. (2014) examined the impact of fluid pulsation frequency and pipeline wall thickness on the dynamic features of fluid pipeline vibration.

Most of the recent research is specialized, theoretical, and based on indoor tests, while little attention has been paid to practical engineering issues. Furthermore, studies tend to focus on systems under 40 MPa. As a result, there is limited understanding of the vibrational properties of the pipe systems used for oilfield plunger pumps that operate at high pressures (e.g., 42–70 MPa). However, water injection pressure levels are moving toward ultra-high pressure due to rising energy demands and the gradual depletion of conventional energy resources. The design of higher-pressure plunger pump injection piping systems currently lacks a theoretical basis and specification because the standard specifications for pipeline design pressure are less than or equal to 42 MPa. Therefore, the present study examined the effects of various parameters on the vibrational characteristics of a high-pressure (42–70 MPa) plunger pump water injection pipeline. The results can guide the design, optimization, and specifications of high-pressure plunger pump water injection pipelines for use in oil and gas fields.

2. ENGINEERING BACKGROUND

Most of the injection pressures of oilfields in China are currently lower than 42 MPa (Ma, 2019). In contrast, plunger pump injection pipes with pressures ranging from 42 to 70 MPa are planned for construction by the Tarim Oilfield Keshen and Kelamayi Gas Field. However, the design of water injection pipelines, fittings, and valves, that operate under pressures greater than 42 MPa no longer satisfy the standard requirements adopted in ground engineering. Therefore, the present study used the Keshen 16 well's existing piping design in the Tarim Oilfield as a model to examine the pipeline's vibrational characteristics under various pressure settings, thereby providing a guide for pipeline design upgrades.

3. RESEARCH METHODOLOGY

The vibrations caused by a plunger pump unit's operation (i.e., promoting water flow through the pipe using vortices, water pulsation, etc.) are more complex than can be accurately determined from established theoretical models. Thus, studies are frequently conducted using fluid-solid coupling numerical simulation methods, which include either one-way or two-way coupling. One-way coupling simply considers the impact of the fluid on the solid, whereas two-way coupling accounts for the mutual impacts. The natural frequencies under one-way coupling are higher than those under two-way coupling, with a difference of 2%–10%, according to Zhou et al. (2022), who studied the two types of coupling in hydraulic pipe systems. In a one-way and two-way coupling analysis of hydraulic turbine blades, Chen et al. (2017) discovered that the impeller should only be subjected to stresses that are up to 2% greater than the deformation variables under one-way coupling conditions. The unidirectional coupling method was ultimately selected for the pipe vibration characteristics investigation in the present work in order to optimize computer performance and time costs.

3.1 Geometric Models

According to the plunger pump water injection pipeline design drawings for the Keshen 16 well, the present study focused on a water injection pipeline between the plunger pump outlet and the wellhead injection port. A three-dimensional model of the water injection pipeline, which has a total length of 36.77 m and a diameter of 114 mm, was created using Spaceclaim software. An internal flow channel model was created using ANSYS Fluent anti-modeling software, with the pipeline's right side serving as the entrance and its left side serving as the exit. The final geometric model is shown in Fig. 1.

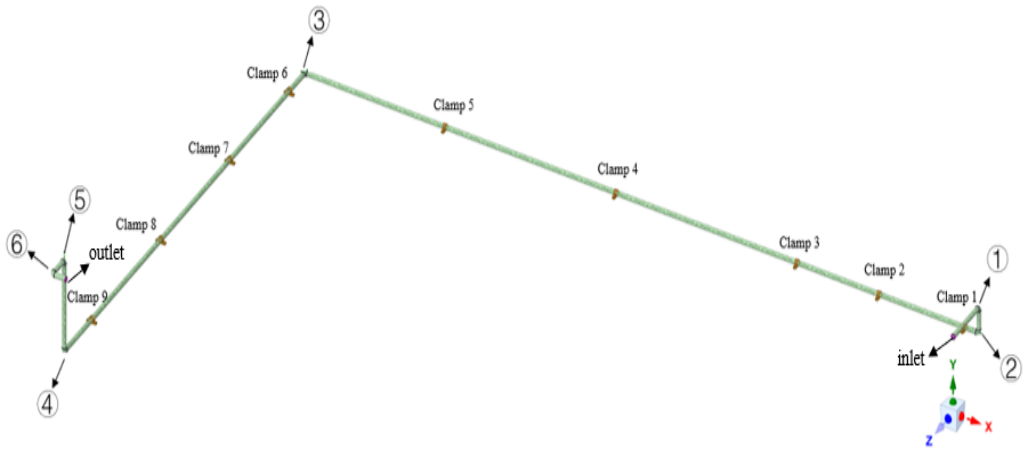

Fig. 1 Schematic diagram of the geometric model

Table 1 Verification of mesh-independence of flow channels in tubes

Grid nodes	Export speed ($m \cdot s^{-1}$)	Outlet flow ($kg \cdot s^{-1}$)
72w	1.325	5.393
77w	1.236	5.436
83w	1.296	5.604
96w	1.282	5.719
115w	1.281	5.775

3.2 Grid and Irrelevance Verification

The mesh independence was verified by outlet average velocity and mass flow rate, which were obtained from calculated flow field using software FLUENT. Table 1 lists the flow rates and velocities at the pipe exit for various mesh sizes.

Table 1 indicates that as the number of grids rises, the velocity and flow rate at the outlet tend to stabilize. The outlet velocity and outlet flow rate are essentially consistent for 83w, 96w, and 115w grids. The grid model with a total of 96w grid cells was selected to minimize processing costs while ensuring a reasonably modest number of grids and limited variation in the solutions.

The fluid medium in this study was continuous liquid water, and the default parameters of liquid water materials in the Fluent material library were used. The standard k-e turbulence model was applied to calculate the transient flow field. The turbulence intensity was 5%. The pressure was set as a sinusoidal pulsation function($P = P_{const} + \sin(\pi \times 30t)$), where the inlet boundary is the pressure inlet, the outlet boundary is the pressure outlet, the amplitude is 1 MPa, and the frequency is π. Take 42MPa for an example, the inlet pressure was set as P_{in}=42+ $\sin(\pi \times 30t)$, and the outlet pressure was P_{outlet}=41.996+$\sin(\pi \times 30t)$. The time step was 0.0005 s, and the wall surface was assumed to be slip-free. The maximum residuals of the continuity, momentum, and turbulence equations were all less than 1.0×10^{-5}.

3.3 Model Validation

A set of in-situ experiments was conducted to measure the vibration of pipelines with Bohua BH550A-II. The sampling frequency was 2000Hz and the number of analysis lines was 1600. Taking various factors into consideration, such as the selection of measurement points, the arrangement of vibration sensors and the distribution type of pipelines, 5 measurement points were uniformly distributed in the middle of elbow ②→③, and 4 measurement points in the middle of the elbow ③→④, as illustrated in Fig. 2. In order to obtain more comprehensive vibration signal data of the pressure pipelines, a three-dimensional coordinate system, namely direction x, y, z, was established along the axial, vertical and radial directions of the pipeline. Taking three vibration sensors as a group, two horizontally and one vertically (as illustrated in Fig. 2), vibration signals were collected at the same time to ensure that the three directions were vibration-related. In order to ensure the accuracy of measurements, six repeated measurements were conducted, and the average displacement in each direction was compared with the simulation results. The modal frequency of pipeline vibration was obtained through time-domain analysis of on-site data signals.

To verify the applicability of the adopted simulation methods, the first six modal frequencies and displacements measured on the Keshen 16 water injection pipeline at 42 MPa were compared with the numerical simulation results, which are listed in Tables 2 and 3, respectively.

Table 2 Frequency simulation results and on-site measurement results

Modal order	Measurements (Hz)	Simulation (Hz)	Relative error (%)
1	16.98	16.480	2.94
2	17.21	16.593	3.59
3	21.01	20.116	4.26
4	21.35	20.646	3.30
5	25.12	24.223	3.57
6	27.52	26.721	2.90

Table 3 Displacement simulation results and on-site measurement results

Direction	Measurements (μm)	Simulation (μm)
x	6.529	6.37
y	31.616	47.17
z	17.675	24.935

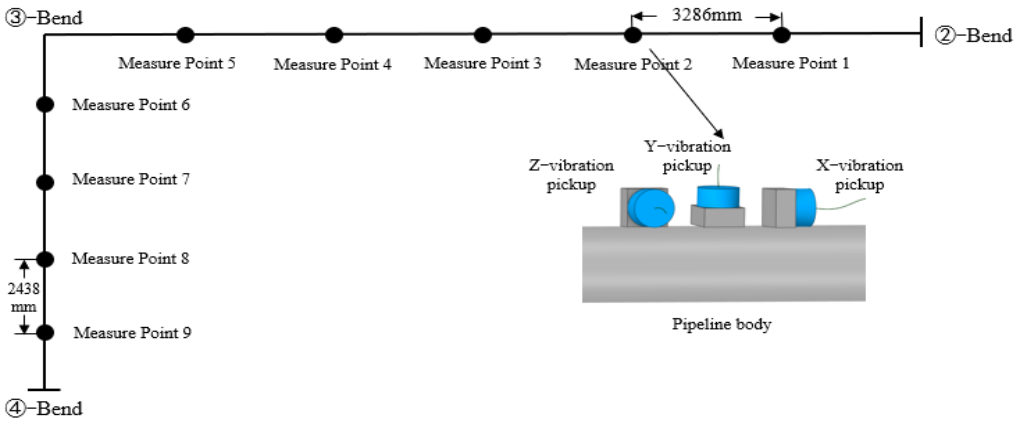

Fig. 2 Location of measuring point and schematic diagram of vibration pickup

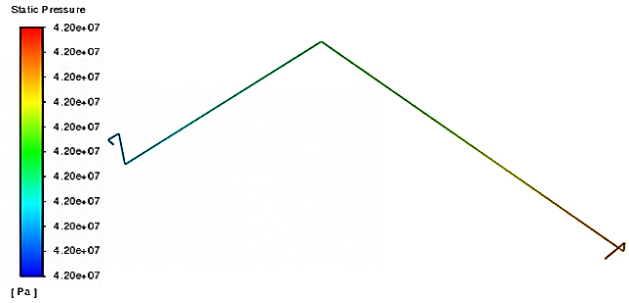

Fig. 3 Imported pressure diagram

The highest frequency error was 4.26%, and the displacement difference did not exceed 20 μm. The on-site measurement results are consistent with the simulation results, thus confirming that the numerical model is reasonable and reliable.

4. VIBRATIONAL ANALYSIS AND CALCULATIONS

4.1 Load Application Method

Because the force at the elbow ① is the largest, the velocity was converted into force and applied at ① to better reflect the vibration of the entire pipeline. According to the Paidoussis & Li (1993), the formula for this calculation is expressed in Eq.(1):

$$F = \rho \times V^2 \times S(1 - cos\theta)^{\frac{1}{2}} \quad (1)$$

where V is the maximum velocity at the elbow (m/s); S is the area of action (m^2), i.e., the projection of the area of the inner arc of the elbow in the direction of the pipe axis. Following this calculation, a force of 48.8 N was applied at ①.

4.2 Vibrational Characteristics of the Pipeline Under Different Pressures

For the simulation analysis, four common pressures (42, 50, 60, and 70 MPa) were selected because of their potential for future operations. In the finite element model, the fluid domain is suppressed, and the pipe wall was meshed. The mesh independence was conducted, and a mesh with 120,000 elements was finally selected for subsequent calculation. The material of the pipe wall was structural steel, and the friction coefficient between the pipe clamp and the pipe was 0.2. The pressure data obtained from the fluid domain calculations were imported into the wall surface to conduct a one-way coupling analysis. The displacement and modal frequency in each direction could then be obtained. Figure 3 shows a schematic diagram of the import pressure.

Table 4 Total displacement under different pressures

Pressure (MPa)	Maximum total displacement (mm)
42	0.91975
50	1.0516
60	1.2144
70	1.3734

The pressure at the inlet was the highest, but as the fluid flows, the pressure gradually decreases due to friction loss and reaches a minimum at the outlet.

Table 4 presents the total displacement of the pipeline vibration when the water injection pipeline's operating pressure is changed, and Fig. 4 shows the maximum displacement of the pipeline in each direction.

As the pipeline operating pressure increases, the total displacement of the pipeline also gradually increases. For example, when the pressure increases from 42 to 50 MPa, the total displacement increases by 14.34%; when it increases from 50 to 60 MPa, displacement increases by 15.48%; and when it increases from 60 to 70 MPa, displacement increases by 13.09%. This phenomenon occurs because when inlet pressure rises, the force of the fluid on the pipe also increases, thereby leading to greater overall displacement.

In general, the displacement increases slightly with increasing pressure. However, the shifting patterns, are contradictory and unpredictable. From 42 to 70 MPa, the displacement in the positive direction increases from 0.51 to 0.61 mm, while the displacement in the negative direction increases from 0.54 to 0.87 mm, corresponding to an increase of up to 61.11%. Along the *x*- and *z*-axes, the growth rate of displacement in the negative direction was significantly greater than that in the positive direction. Positive displacement increased from 0.54 to 0.60 mm when the pressure increased from 42 to 70 MPa, while negative displacement increased from 0.73 to 1.18 mm, corresponding to a growth rate of 61.64%. Although the displacement in the negative direction increased with increasing pressure along the *y*-axis direction, this

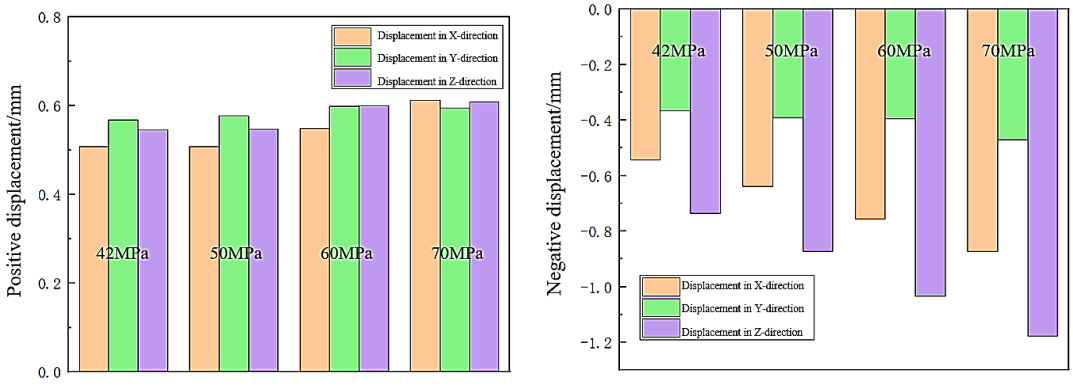

(a) (b)

Fig. 4 Maximum total (a) positive and (b) negative displacement under different pressures

Table 5 Modal frequencies at different pressures

Modal order	1	2	3	4	5	6
42 MPa	16.48	16.593	20.116	20.646	24.223	26.721
50 MPa	16.416	16.535	20.071	20.586	24.207	26.739
60 MPa	16.314	16.433	20.016	20.481	24.219	26.754
70 MPa	15.998	16.164	19.935	20.415	24.165	26.777

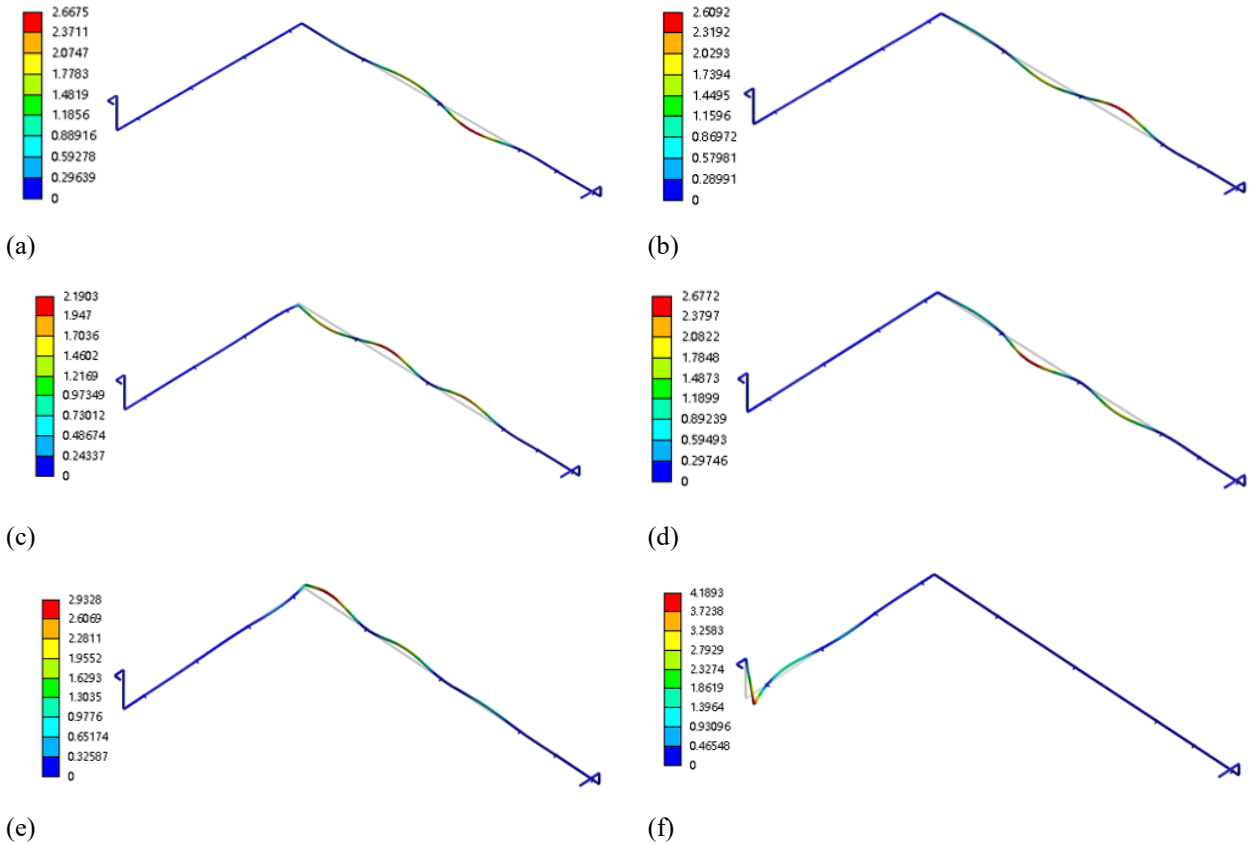

Fig. 5 (a) First-order, (b) second-order, (c) third-order, (d) fourth-order, (e) fifth-order, and (f) sixth-order modal vibration diagrams

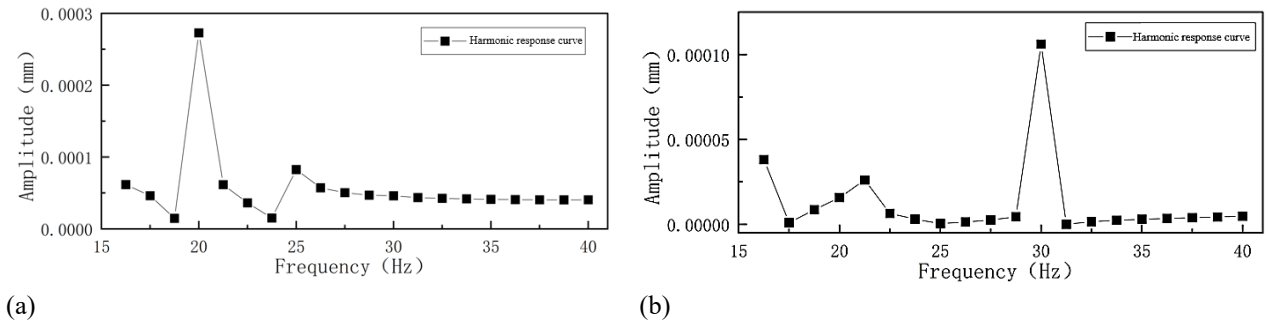

Fig. 6 Harmonic response curves along the (a) *y*-axis and (b) *z*-axis at 42 MPa inlet pressure

increment was much smaller than the changes along the *x*- and *z*-axes. Specifically, when the pressure increased from 42 to 70 MPa, the displacement in the negative direction only increased from 0.37 to 0.47 mm, corresponding to an increase of 27.02%. In contrast, there was a negligible change in the displacement in the positive direction with increasing pressure.

As shown in Table 5, the inherent frequency of the pipe decreased very slightly as the pressure increased, and as the modal order increased, it is reasonable to conclude that the pressure had little to no impact on the inherent frequency.

Figure 5 shows the total displacement(mm) in the first six modes, and Fig. 6 shows the harmonic response curves in the *y*- and *z*-directions. The extreme value frequency of fluid pulsation in the *y*-direction at 42 MPa is closest to

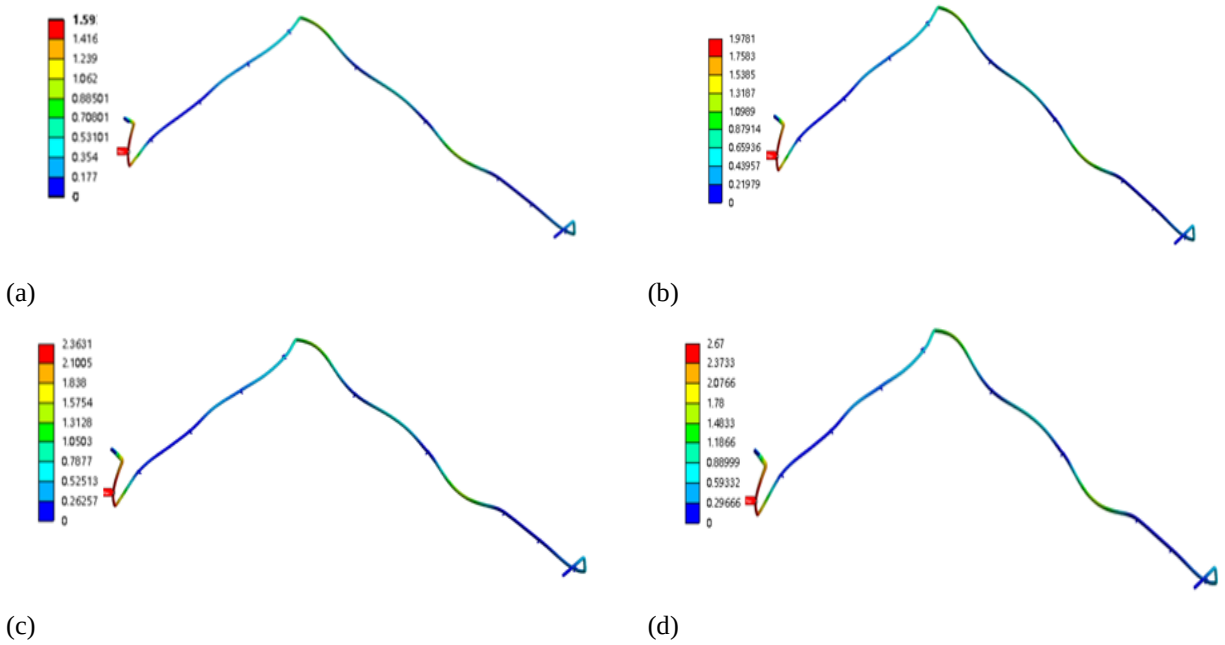

Fig. 7 Total displacement under (a) 42, (b) 50, (c) 60, and (d) 70 MPa

the third-, fourth-, and fifth-order modes, whereas the extreme value frequency in the *z*-direction is closest to the fourth mode frequency.

Typically, low-frequency vibrations are more likely to occur at the pipeline between locations ② and ③ when combined with the first- to sixth-order mode vibration diagrams (see Fig. 5). These results also demonstrate that resonance is expected to occur in the same places, regardless of the pressure. Figure 7 shows the total displacement under different pressures. The position of the maximum displacement remains consistent as the inlet pressure increases, which supports the aforementioned conclusion.

4.3 Pipeline Vibrational Characteristics for Different Pipe Lengths and Pipe Clamp Schemes

To establish a foundation for the appropriate setting of pipe clamps for high-pressure fluid pipelines, the impact of various pipe lengths on the inherent frequency of the pipe was investigated. A total of 3, 4, 5, or 6 clamps were placed 400 mm from the elbow of 2 to 3 pipes and evenly spaced and separated in the middle. The parameter settings were the same as those shown in Fig. 1, and the schematic diagram of four pipe clamps for a 6-m pipeline is shown in Fig.8.

The inherent frequencies at 6, 9, and 12 m for various numbers of pipe clamps under 42 MPa are displayed in Tables 7, 8, and 9, respectively.

Tables 7, 8, and 9 show that the inherent frequency of the pipe gradually increases with increasing numbers of pipe clamps, although the magnitude of the increase gradually declines at the same pressure and pipe length. Taking the first-order inherent frequency of a 6-m long pipe as an example, the inherent frequency doubles when the number of pipe clamps is increased from 3 to 4, increases by 52.76% when the number of pipe clamps is increased from 4 to 5, and increases by 9.45% when the number of pipe clamps is increased from 5 to 6. Moreover, as the tube length increases, the inherent frequency of each order decreases.

These findings indicate that the intrinsic frequency of the pipe vibration is significantly influenced by the pipe length, the number of clamps, and the placement of those clamps. Modifying the number and placement of clamps represents an efficient approach to reduce the pipe vibrations; however, in practicality, the pipe length is frequently constrained by the field variables.

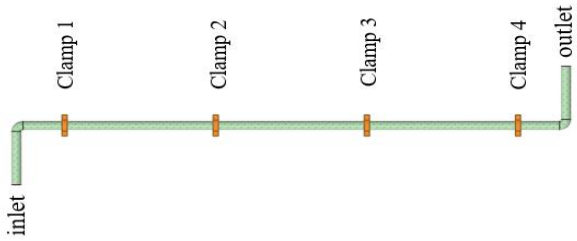

Fig. 8 Schematic diagram of a 6-m pipe with 4 pipe Clamps

Table 7 Intrinsic frequency of a 3-m pipe with different numbers of pipe clamps

Modal order	1	2	3	4	5	6
3 pipe clamps	67.641	69.699	81.279	83.898	186.33	200.72
4 pipe clamps	135.28	137.73	152.46	161.69	180.1	186.54
5 pipe clamps	206.66	210.29	225.07	242.16	253.31	275.52
6 pipe clamps	226.19	226.75	332.61	342.4	361.12	375.06

Table 8 Intrinsic frequency of a 6-m pipe with different numbers of pipe clamps

Modal order	1	2	3	4	5	6
3 pipe clamps	24.789	26.427	31.753	33.61	74.259	79.05
4 pipe clamps	42.288	43.243	49.222	59.547	62.769	73.572
5 pipe clamps	75.823	79.809	89.473	95.985	108.88	117.59
6 pipe clamps	104.49	108.44	112.24	118.06	129.95	140.28

Table 9 Intrinsic frequency of a 12-m pipe with different numbers of pipe clamps

Modal order	1	2	3	4	5	6
3 pipe clamps	15.677	15.848	18.271	18.721	45.215	45.858
4 pipe clamps	31.771	32.085	36.691	37.537	41.792	42.469
5 pipe clamps	52.302	53.325	59.141	59.684	67.203	68.686
6 pipe clamps	77.288	79.103	85.603	85.647	95.515	97.22

4.4 Optimized Solutions

Field practice is used as the benchmark to ensure that the pipeline length remains constant while altering the number and location of the intermediate pipe clamps to avoid the resonance interval.

4.4.1 Results After Optimizing A 42 Mpa Field Pipeline

The number and placement of the pipe clamps in this study were modified considering the fact that the first six steps of the 42 MPa vibration pattern revealed that the pipe vibrations occurred primarily between ② and ③. A fixed pipe clamp was positioned 400 mm from elbows ② and ③, and clamps 3, 5, and 7 were spaced equally apart in the middle section. As an illustration, consider the optimized system comprising 9 pipe clamps (front view displayed in Fig. 9). Here, only the ② and ③ interblend clamp is optimized, and only the clamp rearrangement of this section is shown. The modal frequencies for various numbers of pipe clamps are shown in Table 5 to help determine the optimal number to use to conserve material.

For the 5-pipe clamp system, the first four modal orders were marginally improved following optimization (Table 10). However, the middle clamps in this case are too far apart, and as a result, the subsequent modal frequencies are lower than those before optimization. Additionally, the harmonic response analysis demonstrated that none of the optimization techniques could completely eliminate the vibrational frequencies. The modal frequency increased appreciably as the number of pipe clamps increased. For example, the first-order modal frequency increased by 46.48% when the number of pipe clamps increased from 5 to 7. The harmonic response analysis curve for the 9-pipe clamp system following optimization is shown in Fig. 10

Fig. 9 Optimized pipe clamp positions

Table 10 Modal frequencies for different numbers of pipe clamps

Modal order	1	2	3	4	5	6
Optimized 5-pipe clamp	18.217	18.428	20.649	20.873	23.458	24.113
Optimized 7-pipe clamp	26.685	34.377	35.375	37.918	38.567	40.925
Optimized 9-pipe clamp	26.673	34.328	35.312	42.201	44.516	46.771

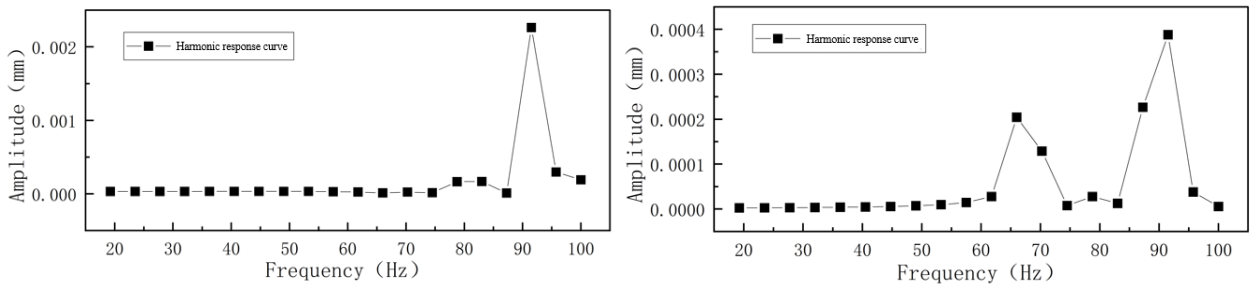

(a) (b)

Fig. 10 Harmonic response curves in the (a) *y*-axis and (b) *z*-axis directions for the 9-pipe clamp system under 42 MPa after optimization

Table 11 Modal frequencies at 50 MPa with different numbers of pipe clamps

Modal order	1	2	3	4	5	6
Optimized 5-pipe clamp	19.02	18.42	20.624	20.782	23.367	24.015
Optimized 7-pipe clamp	26.701	34.32	35.336	37.888	38.504	40.912
Optimized 9-pipe clamp	26.691	34.315	35.326	42.21	44.502	46.767

Table 12 Modal frequencies at 60 MPa with different numbers of pipe clamps

Modal order	1	2	3	4	5	6
Optimized 5-pipe clamp	18.064	18.28	20.518	20.757	23.327	23.997
Optimized 7-pipe clamp	26.723	34.247	35.291	37.903	38.434	40.922
Optimized 9-pipe clamp	26.712	34.242	35.27	42.159	44.438	46.741

Table 13 Modal frequencies at 70 MPa with different numbers of pipe clamps

Modal order	1	2	3	4	5	6
Optimized 5-pipe clamp	17.971	18.18	20.439	20.679	23.247	23.916
Optimized 7-pipe clamp	26.759	34.174	35.32	37.846	38.351	40.87
Optimized 9-pipe clamp	26.734	34.167	35.228	42.104	44.374	46.714

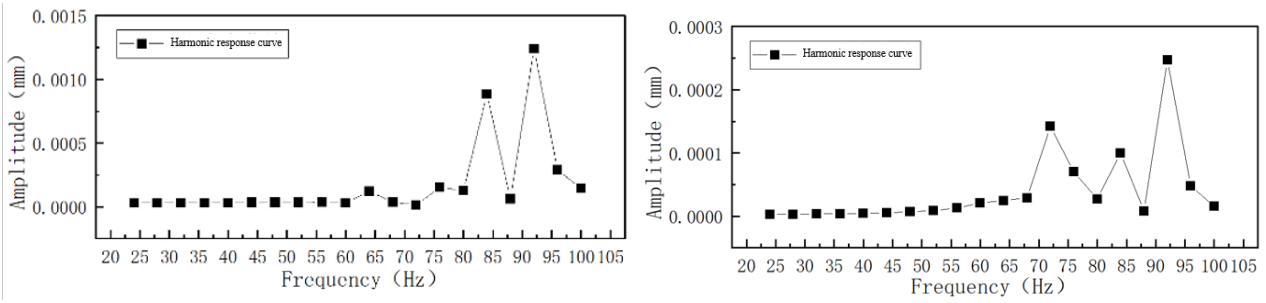

(a) (b)

Fig. 11 Harmonic response curves in the (a) *y*-axis and (b) *z*-axis directions for a 9-pipe clamp system under 70 MPa after optimization

These results demonstrated that resonance is more likely to occur at 65 and 90 Hz when there are 9 pipe clamps. When the first sixth-order modal frequency is avoided at this moment, resonance can be prevented efficiently.

4.4.2 Optimized Results for Field Pipes at Different Pressures

The inherent frequencies of the pipes after optimization at various pressures are shown in Tables 11 to 13. The influence of the number of clamps on the pipeline's intrinsic frequency is consistent across the tested pressure range (i.e., 42–70 MPa). The inherent frequencies of the pipeline's first six orders all rose appreciably when the number of pipe clamps increased from 5 to 7. The pipeline's first three natural frequencies varied slightly when the number of clamps was increased from 7 to 9, while the fourth to sixth orders increased considerably.

According to the harmonic response study, the resonance interval may be effectively avoided when 9 pipe clamps are installed in the 17.6-m straight pipe section when the injection line pressure is 42, 50, 60, or 70 MPa. Figure 11 shows the harmonic response curves at 70 MPa along the *y*- and z-axes. As depicted in Fig.9, when 9 pipe clamps were installed in the investigated pipe section, the resonant frequency in the *y*-direction ranged from 80 to 100 Hz, while the resonant frequency in the *z*-direction ranged from 70 to 95 Hz. By avoiding the first six orders of the pipe's inherent frequency, this effectively prevented the occurrence of resonance.

5. CONCLUSIONS

Herein, a one-way coupling method was adopted to investigate the vibrational characteristics of a water injection pipeline under ultra-high pressure. The following conclusions can be drawn from the result of this study:

(1) Under high-pressure conditions, the total displacement of the pipeline and the displacement in each direction increase with increasing pressure, while the modal frequency decreases. The main displacement position of the pipe section is at the elbow. It is therefore necessary to apply additional pipe clamps near the elbow in practical engineering applications.

(2) The harmonic response analytical method was used to analyze the possible resonant frequencies, revealing that the vibrations occur mainly between ② and ③ in the investigated pipe system. The position and number of pipe clamps were adjusted, and the modal frequency increased gradually with increasing numbers of pipe clamps.

(3) When the pressure is between 42 and 70 MPa, it is possible to avoid resonance by using the optimum scheme

of a fixed pipe clamp 400 mm from the existing pipe section's elbow and additional pipe clamps spaced 2365 mm apart in the straight middle pipe section.

The present work focused on existing pipelines on site, and thus, the applicability of the obtained results is somewhat limited. In addition, a relatively simple numerical method was used for the optimization study. In future work, more complex and comprehensive optimization algorithms, such as genetic algorithms or particle swarm optimization methods, can be adopted to obtain more universal laws.

CONFLICTS OF INTEREST

No potential conflict of interest was reported by the authors.

AUTHOR CONTRIBUTIONS

Dongyin Yan: Writing – original draft; **Cunyang Zhang**: Project administration; **Chao Wang**: Computation; **Tao Zhang**: Methodology; **Chiyu Wang**: Formal analysis; **Fengzhi Sun**: Writing – review & editing.

REFERENCES

Ashley, H., & Haviland, G. (1950). Bending vibrations of a pipeline containing flowing fluid. *Journal of Applied Mechanics*, *17*, 229-232. https://doi.org/10.1115/1.4010122

Azizian, R., & Torrado, P. A. (2016). Practical *Approach to mitigate the excessive vibration of a piping system subjected to flow-induced excitation*. ASME Pressure Vessel Piping Conference. https://doi.org/10.1115/PVP2016-63088

Benjamin, T. B. (1961). *Dynamics of a system of articulated pipes conveying fluid, I: Theory.* Proceedings of the Royal Society (London), A261, 457-486. https://doi.org/10.1098/rspa.1961.0090

Chen, Z., Zhang, G., Zhao, Z., Chen, J., & Zhen, W. (2017). Analysis of pressure fluctuation characteristics of tidal energy turbine impeller. *Vibration and Shock*, *36*(19), 98-105. https://doi.org/10.13465/j.cnki.jvs.2017.19.015

Finnveden, S. (1997). Spectral finite element analysis straight fluid-filled pipes with flanges. *Journal of Sound and Vibration*, *199*(1), l25-154. https://doi.org/10.1006/jsvi.1996.0602

Gregory, R. W., & Paidoussis, M. P. (1996). Unstable oscillation of tubular cantilevers conveying fluid-I theory. *Proceedings of The Royal Society A. 293*(5), 512-527. https://doi.org/10.1098/rspa.1966.0188

Housner, G. W. (1952). Bending vibrations of a pipeline containing flowing fluid. *Applied Mechanics*, *19*, 205-208. https://doi.org/10.1115/1.4010447

Lee, U., Pak, C. H., & Hong, S. C. (1995). The dynamics of a piping system with internal unsteady flow. *Journal of Sound and Vibration*, *180*(2), 297-311. https://doi.org/10.1006/jsvi.1995.0080

Li, S., Lei, B., & Li, Y. (2012). Modal analysis of pipeline vibration under fluid structure coupling Forging Equipment and Manufacturing Technology, *47*(04), 76-78. https://doi.org/10.16316/j.issn.1672-0121.2012.04.009

Long, R. H. (1955). Experimental and theoretical study of transverse vibration of a tube containing flowing fluid. *Journal of Applied Mechanics*, *22*(6),65-68. https://doi.org/10.1115/1.4010971

Ma, K. (2019). *The research of plunger pump outlet pipeline vibration*. Beijing, China University of Petroleum Beijing. https://doi.org/10.27643/d.cnki.gsybu.2019.000706

Miwa, S., Mori, M., & Hibiki, T. (2015). Two-phase flow induced vibration in piping systems. *Progress in Nuclear Energy*, 78270-284. https://doi.org/10.1016/j.pnucene.2014.10.003

Paidoussis, M. P. (2008). The canonical problem of the fluid-conveying pipe and radiation of the knowledge gained to other dynamics problems across applied mechanics. *Journal of Sound and Vibration*, *310*(3), 462-492. https://doi.org/10.1243/JMES_JOUR_1976_018_034_02

Paidoussis, M. P., & Laithier, B. E. (1976). Dynamic of timoshenko beams conveying fluid. *Journal of Mechanical Engineering Science*, *18*(4), 210-220. https://doi.org/10.1243/JMES_JOUR_1976_018_034_02

Paidoussis, M. P., & Li, G. X. (1993). Pipes conveying fluid: A model dynamical problems . *Journal of Fluids and Structure*, 7137-204 . https://doi.org/10.1006/jfls.1993.1011

Sarkar, A., & Paidoussis, M. P. (2004). A cantilever conveying fluid: coherent modes versus beam modes. *International Journal of Non-Linear Mechanics*, *39*(3), 467-481. https://doi.org/10.1016/S0020-7462(02)00213-5

Sunil, K., & Raghunandana, K. (2014). Vibration analysis of a piping system attached with pumps and subjected to resonance. *Ihternational Journal of Emerging Technology and Advanced Engineering*, *4*(9),1-6.

Tijsseling, A. S. (2007). Water hammer with fluid–structure interaction in thick-walled pipes. *Computers & Structures*, *85*(11), 844-851. https://doi.org/10.1016/j.compstruc.2007.01.008

Xie, A., Ke, Y., L, S., & Zhou, H. (2014). Analysis of vibration characteristics of hydraulic pipelines under pulsating flow excitation. *Hydraulic and Pneumatic*, (09), 117-120. https://doi.org/10.11832/j.issn.1000 − 4858.2014.09.028

Yang, J., Preidikman, S., & Balaras, E. (2008). A strongly coupled, embedded-boundary method for fluid–structure interactions of elastically mounted rigid bodies. *Journal of Fluids and Structures*, *24*(2), 167-182. https://doi.org/10.1016/j.jfluidstructs.2007.08.002

Zhi, C. O., Eng, H. C., & Noroozi, S. (2016). Non-destructive testing and assessment of a piping system with excessive vibration and recurrence crack issue: An industrial case study. *Engineering Failure Analysis*, S1350630716306653. https://doi.org/10.1016/j.engfailanal.2016.12.007

Zhou, X., Lv, K., Zhou, S., & Guo, W. (2022). Analysis of vibration characteristics of hydraulic pipeline system on rolling vibration test bench. *Noise and Vibration Control*, *42* (01), 56-60. https://doi.org/10.3969/j.issn.1006-1355.2022.01.009